



Synthesis of highly tetragonal BaTiO₃ nanopowders by a two-step alkoxide–hydroxide route

Mi-Ri Joung^a, Jin-Seong Kim^a, Myung-Eun Song^a, Jae-Hong Choi^a, Sahn Nahm^{a,*}, Chang-Hak Choi^b, Tae-Hyun Sung^c

^a Department of Materials Science and Engineering, Korea University, 1-5 Ka, Anam-Dong, Sungbuk-Ku, Seoul 136-701, Republic of Korea

^b LCR Division, Samsung Electro-Mechanics Co., 314, Maetan3-Dong, Yeongtong-Gu, Suwon, Gyeonggi-Do 443-743, Republic of Korea

^c Department of Electric Engineering, Hanyang University, 222, Wangsimni-ro, Seongdong-Gu, Seoul 133-791, Republic of Korea

ARTICLE INFO

Article history:

Received 2 September 2010

Accepted 14 June 2011

Available online 1 July 2011

Keywords:

Nanostructured materials

Chemical synthesis

Nanopowders

ABSTRACT

BaTiO₃ (BT) nanopowders were synthesized using the alkoxide–hydroxide route. Formation of BT nanopowders commenced at 60 °C and their amount increased with increasing temperature. However, a TiO₂ second phase was always developed at temperatures higher than 100 °C due to the insufficient amount of H₂O caused by its evaporation. Therefore, a two-step process is presented herein for the synthesis of homogeneous, highly tetragonal BT nanopowders. The cubic BT nanopowders were synthesized at 100 °C and subsequently heated to high temperatures (>200 °C) to increase their tetragonality. Homogeneous BT nanopowders with an average size of 94.8 nm and a high *c/a* ratio of 1.0081 were obtained for the specimens synthesized at 260 °C for 60 h after the formation of the cubic BT nanopowders at 100 °C for 20 h.

© 2011 Elsevier B.V. All rights reserved.

1. Introduction

BaTiO₃ (BT) ceramics have been widely used in the electric components such as multilayer ceramic capacitors (MLCCs), piezoelectric sensors, and positive temperature coefficient of resistance and electro-optical devices because of their excellent dielectric, piezoelectric and ferroelectric properties [1–4]. Recently, electronic devices such as MLCCs have been miniaturized to cope with the high integration of microelectronic devices. In order to shrink large-capacitance MLCCs, the thickness of the MLCC's dielectric layer should be decreased, for example by decreasing the size of the BT powders. The thickness of the dielectric layer has been reduced to 0.6 μm by using 0.15 μm-sized BT powders. However, the dielectric layer needs to be further decreased to 0.5 μm, which necessitates the use of highly tetragonal BT nanopowders smaller than 100 nm.

The hydrothermal method has been used to produce BT nanopowders with a narrow particle size distribution at low temperature [5–7]. However, the BT nanopowders formed by the hydrothermal method exhibit low tetragonality and contain hydroxyl ions in oxygen sites, which produces a moisture gas during the heat treatment, thereby causing MLCC failure [8]. Sol–gel processes have also been used to produce BT nanopowders, but the amorphous or precursor phases that were produced necessi-

tated heating at high temperature in order to form the crystalline BT phase. The alkoxide–hydroxide method, first suggested by Flashen, has been extensively investigated for the synthesis of the BT nanopowders because crystalline BT nanopowders are easily produced at temperatures lower than 100 °C [9]. However, most studies focused on the initial stage of the formation of crystalline BT nanopowders at low temperatures (≤100 °C). Therefore, the BT nanopowders formed by the alkoxide–hydroxide route showed relatively low tetragonality [10–15]. For high-capacitance MLCCs, BT nanopowders require a high tetragonality (*c/a* ≥ 1.008) and a small particle size (≤100.0 nm) in order to form thin dielectric layers (<0.5 μm). However, for the BT nanopowders formed at high temperatures, a TiO₂ second phase was always formed. In this work, therefore, a new, two-step process was suggested for the first time for the synthesis of homogeneous, highly tetragonal BT nanopowders.

2. Experimental procedure

BT nanopowders were prepared by the alkoxide–hydroxide route using barium hydroxide octahydrate (Ba(OH)₂·8H₂O, reagent grades, Junsei Chemical Co., Ltd., Japan), and titanium (IV) isopropoxide (Ti[OCH(CH₃)₂]₄, 99.999%, Aldrich). These starting raw materials were placed inside a Teflon-lined vessel and mixed with 2-methoxyethanol (CH₃OCH₂CH₂OH, 99.8%, Aldrich) as a solvent at room temperature with various Ba/Ti ratios (1.0–2.0). The total volume of the mixture was 70% of the vessel capacity. They were heated to 100 °C and held for 20 h for the formation of the BT nanopowders having a cubic structure, and subsequently heated to various temperatures (200–260 °C) for various periods (20–60 h) in an oven. The resulting BT powders were filtered and washed with distilled water, and finally oven dried at 70 °C for 12 h to afford white colored BT nanopowders. The structural properties of

* Corresponding author. Tel.: +82 2 3290 3279; fax: +82 2 928 3584.

E-mail address: snahm@korea.ac.kr (S. Nahm).

the specimens were examined by X-ray diffraction (XRD; Rigaku D/max-RC, Tokyo, Japan). For a wide range of XRD measurement from 20° to 60° , the scan rate was $5^\circ/\text{min}$ and a slow scan rate of $0.1^\circ/\text{min}$ was used for a specific range from 44° to 46° . The a and c lattice constants were obtained from the (200) and (002) reflections, respectively, and the tetragonality (c/a ratio) was calculated from these peaks. For the Rietveld refinement, XRD patterns were also taken from 20° to 145° with a step length of 0.02° and a fixed counting time of 2 s and the Rietan-2000 program was used to determine the tetragonality of the BT nanopowders. The average particle size and morphology of the nanoparticles were determined by scanning electron microscopy (SEM; Hitachi S-4300, Osaka, Japan). The average particle size of the powders was also calculated using the Brunauer–Emmett–Teller (BET) specific surface area measured by Tristar 3000 (Micromeritics Co. Ltd., USA).

3. Results and discussion

Fig. 1a–e shows the XRD patterns of the BT nanopowders formed at various temperatures with a Ba/Ti ratio of 2.0. Peaks for the BT phase had already been found in the specimen synthesized at 60°C and their intensity increased with increasing temperature. Moreover, the peak intensity for the BaCO_3 phase decreased with increasing temperature. No splitting of the (002) and (200) peaks at $2\theta \sim 45^\circ$ was observed, indicating that the structure of specimens was close to the cubic BT phase. A peak for the TiO_2 phase, indicated by the arrow, was found for the specimens synthesized above 100°C and the TiO_2 second phase already existed in the specimen synthesized at 100°C with a Ba/Ti ratio of 1.0, as shown in Fig. 1f. On the other hand, no TiO_2 second phase was formed when the H_2O was intentionally added, which will be discussed in later, indicating that the formation of TiO_2 second phase could be related to the amount of H_2O . In general, the formation rate and the yield of BT nanopowders are considerably influenced by the hydroxyl concentration and pH, which are closely related to the amount of H_2O [16]. Therefore, the formation of the TiO_2 second phase could be explained by the decreased hydroxyl concentration and pH of the solution, due to the evaporation of H_2O at high temperature. Moreover, according to the previous work, the BT phase is formed by hydrolysis and condensation processes according to the following equations [14].

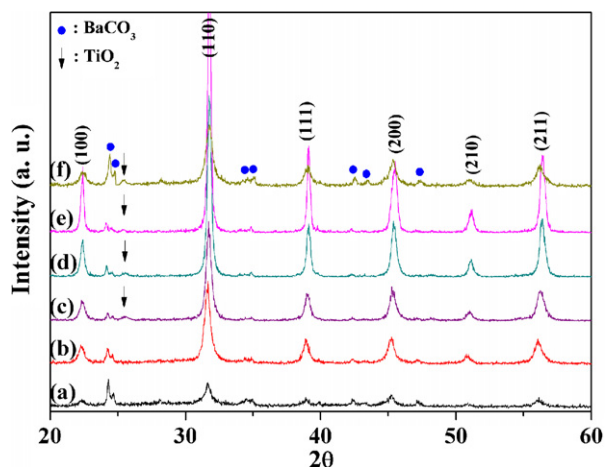
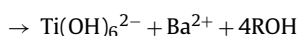
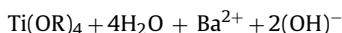


Fig. 1. XRD patterns of the BT nanopowders synthesized at the following temperatures with a Ba/Ti ratio of 2.0: (a) 60°C , (b) 100°C , (c) 130°C , (d) 160°C , (e) 200°C , and (f) at 100°C with a Ba/Ti ratio of 1.0.

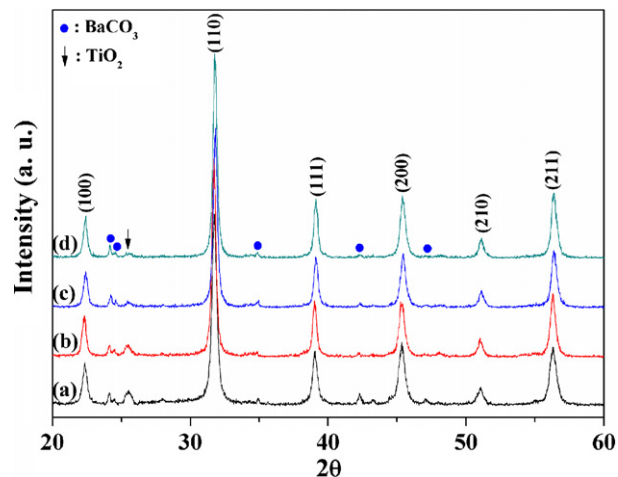
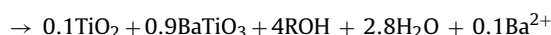
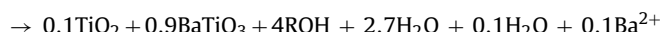
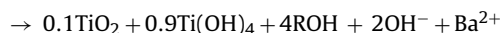
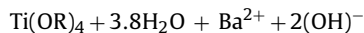


Fig. 2. XRD patterns of the BT nanopowders synthesized at 160°C with the following Ba/Ti ratios: (a) 1.3, (b) 1.5, (c) 1.7 and (d) 2.0.

where R represents an alkoxide group. Therefore, it is also possible that the shortage of H_2O due to the evaporation contributed to the formation of TiO_2 second phase, as shown in following equations:



where the remnant Ba^{2+} ions are considered to interact with CO_2 in air to form the BaCO_3 .

To investigate the effect of H_2O on the TiO_2 second phase formation, BT nanopowders were synthesized at 160°C with various Ba/Ti ratios (1.3–2.0) and their XRD patterns are shown in Fig. 2a–d. The amount of TiO_2 phase decreased with increasing Ba/Ti ratio, probably due to the increased amount of H_2O with increasing $\text{Ba}(\text{OH})_2 \cdot 8\text{H}_2\text{O}$ content. This indicated that the TiO_2 second phase formation was related to the amount of H_2O . Water was intentionally added during the hydrolysis process to confirm the relation between its amount and the TiO_2 second phase formation. Fig. 3

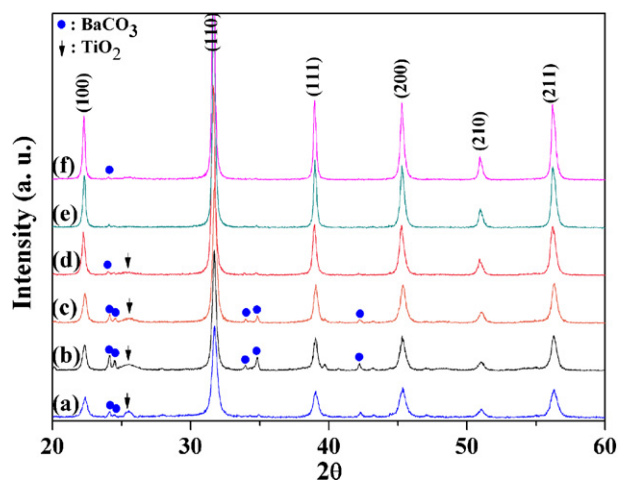


Fig. 3. XRD patterns of the BT nanopowders synthesized at 160°C with the following amounts of H_2O and a Ba/Ti ratio of 1.3: (a) 0.0 mol.%, (b) 0.05 mol.%, (c) 0.1 mol.%, (d) 0.2 mol.%, (e) 0.4 mol.% and (f) 0.5 mol.%.

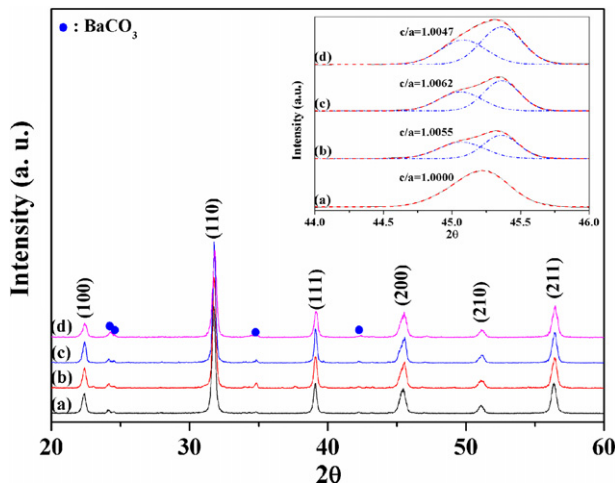


Fig. 4. XRD patterns of the BT nanopowders synthesized at the following temperatures for 20 h after the formation of cubic BT nanopowders at 100 °C with a Ba/Ti ratio of 2.0: (a) 200 °C, (b) 240 °C and (c) 260 °C, and (d) synthesized at 240 °C for 20 h after the formation of cubic BT nanopowders at 60 °C. The inset shows a peak at around $2\theta = 44\text{--}46^\circ$ deconvoluted into (002) and (200) peaks and the c/a ratio obtained from these peaks.

shows the XRD patterns of the BT nanopowders synthesized at 160 °C with various amounts of H_2O with a constant Ba/Ti ratio of 1.3. When the amount of H_2O exceeded 0.2 mol.%, the peak for the TiO_2 second phase disappeared. These results indicate that the shortage of water was responsible for the formation of TiO_2 second phase. BT nanopowders with a high tetragonality ($c/a \geq 1.008$) are generally obtained at temperatures higher than 200 °C. Therefore, TiO_2 second phase formation seems to be unavoidable in the absence of water for the synthesis of highly tetragonal BT nanopowders. However, the use of water in the synthesis of the BT nanopowders makes it difficult to control the shape and size of the BT nanopowders. A large amount of the $\text{Ba}(\text{OH})_2 \cdot 8\text{H}_2\text{O}$ (high Ba/Ti ratio) can be used to produce tetragonal BT nanopowders without the TiO_2 second phase, but the BT nanopowders became agglomerated when the Ba/Ti ratio exceeded 2.0. Therefore, a new method is required for the synthesis of homogeneous, highly tetragonal BT nanopowders using the alkoxide–hydroxide route.

According to the above results, BT nanopowders with a cubic structure were formed at temperatures lower than 100 °C, without the formation of any TiO_2 second phase. Therefore, if these cubic-

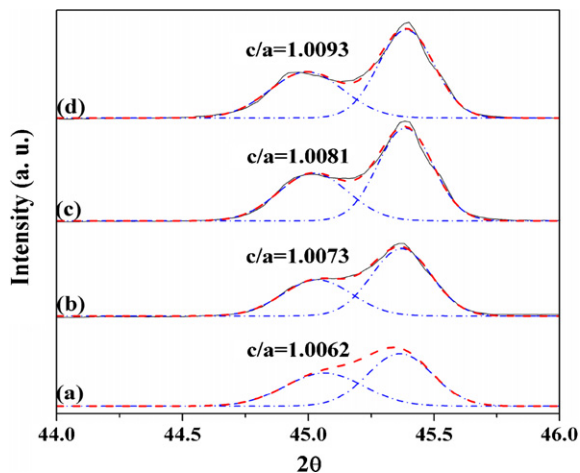


Fig. 5. XRD patterns measured using a slow scan around $2\theta = 44\text{--}46^\circ$ for the BT nanopowders produced at 260 °C for the following times after the formation of cubic BT nanopowders at 100 °C: (a) 20 h, (b) 40 h, (c) 60 h and (d) 80 h.

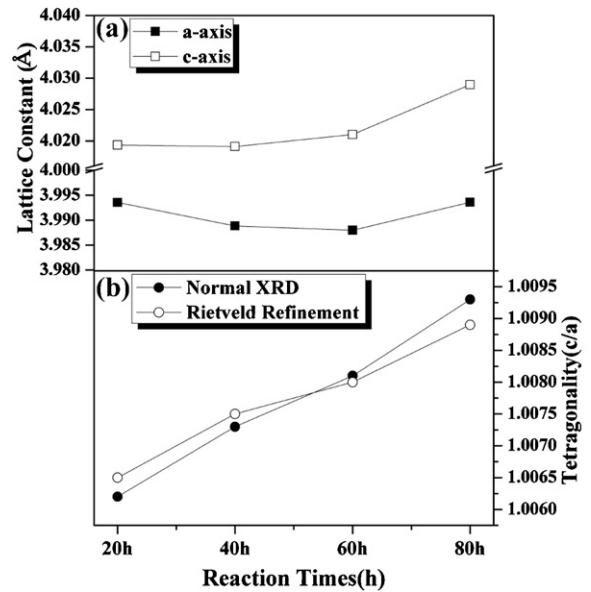


Fig. 6. (a) Lattice constants and (b) c/a ratio obtained from Rietveld refinement for the BT nanopowders produced at 260 °C for various times after the formation of cubic BT nanopowders at 100 °C.

structure BT nanopowders were subsequently heated to higher temperatures ($\geq 200^\circ\text{C}$), homogeneous BT nanopowders with a tetragonal structure could be obtained. All the cubic BT nanopowders were formed at 100 °C because the BT nanopowders formed at 100 °C showed the largest c/a ratio after high-temperature heating, as discussed below. Fig. 4 shows the XRD patterns of the BT nanopowders synthesized at various temperatures for 20 h after the formation of cubic BT nanopowders at 100 °C with a Ba/Ti ratio of 2.0. A homogeneous BT phase was well developed in all the specimens without any TiO_2 second phase. The inset shows a peak at around $2\theta = 44\text{--}46^\circ$ deconvoluted into (002) and (200) peaks and the c/a ratios of the specimens shown in Fig. 4. For the specimen synthesized at 200 °C, the c/a ratio was small at approximately 1.000 but increased with increasing temperature to 1.0062 for the nanopowders synthesized at 260 °C. The XRD pattern and c/a ratio of the BT nanopowders, which were formed at 60 °C and subsequently heated to 240 °C, are also shown in Fig. 4d and in the inset of Fig. 4, respectively. Compared to the c/a ratio of the BT nanopowders formed at 100 °C and synthesized at 240 °C (~ 1.0055), they showed a smaller c/a ratio of 1.0047, probably due to their smaller powder size.

In order to further increase the tetragonality of the specimens, BT nanopowders formed at 100 °C with a Ba/Ti ratio of 2.0 were synthesized at 260 °C for various times, as shown in Fig. 5a–d. The c/a ratio of the BT nanopowders increased with increasing heating time from approximately 1.0062 for 20 h synthesis to 1.0093 for 80 h synthesis. The BT nanopowders synthesized for 60 h also showed a high c/a ratio of 1.0081. In order to confirm the tetragonality of these nanopowders, Rietveld analysis was also conducted on these specimens and their lattice constants and the tetragonality are shown in Fig. 6a and b, respectively. The c/a ratio obtained by the Rietveld analysis was very similar to that obtained from Fig. 5.

Fig. 7a–d shows the SEM images of the BT nanopowders formed at 100 °C with a Ba/Ti ratio of 2.0 synthesized at 260 °C for various times. The particle size of the BT nanopowders increased with increasing heating time from approximately 65.4 nm for 20 h synthesis to 128.6 nm for 80 h synthesis. The size of the BT nanopowders, as equivalent spherical diameter, was also calculated from the BET specific surface area using the equation, $d_{\text{BET}} = 6/(\rho S_{\text{BET}})$, where ρ is the density and S_{BET} the specific sur-

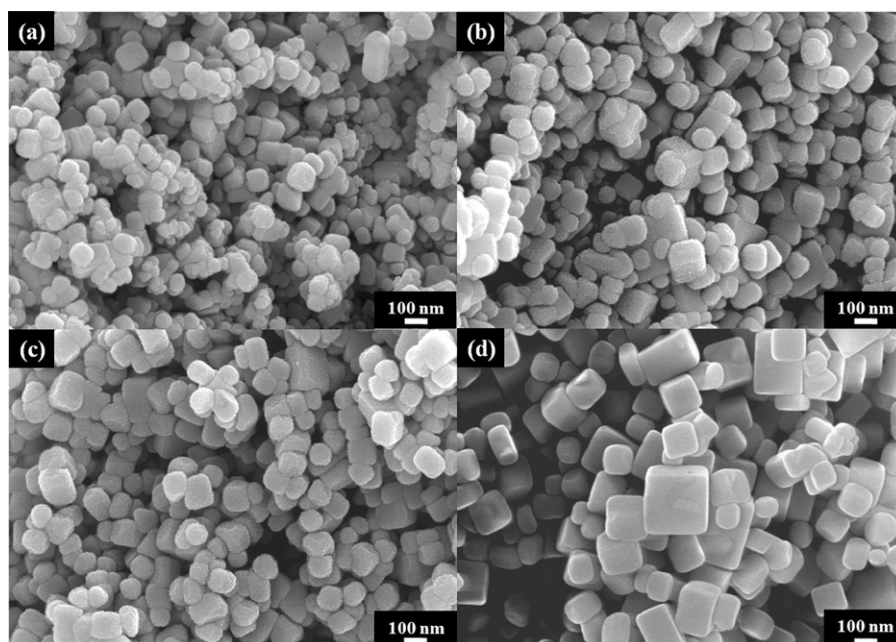


Fig. 7. SEM images of the BT nanopowders formed at 100 °C with a Ba/Ti ratio of 2.0 and subsequently heated to 260 °C for the following times: (a) 20 h, (b) 40 h, (c) 60 h and (d) 80 h.

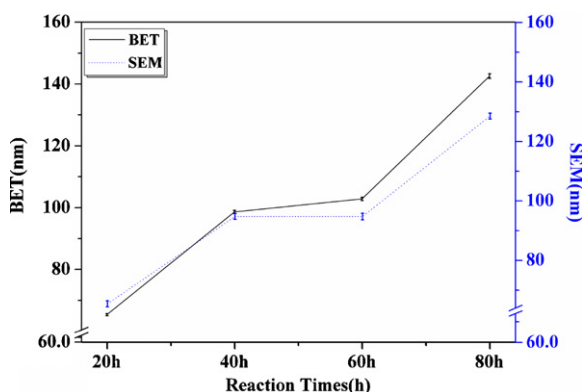


Fig. 8. Size of the BT nanopowders obtained from SEM images and measured specific surface area. These BT nanopowders were produced at 260 °C for various times after the formation of cubic BT nanopowders at 100 °C.

face area. The sizes of the BT nanopowders obtained by both SEM and BET specific surface area are shown in Fig. 8. The latter measurement was slightly larger than the former for the specimens synthesized for more than 20 h but the difference was not significant. In particular, the d_{BET} of the BT nanopowders synthesized for 60 h at 260 °C, which had a high c/a ratio of 1.0081, was approximately 102.84 nm, indicating that the size of the BT nanopowders synthesized at 260 °C for 60 h was close to 100 nm.

4. Conclusions

BT nanopowders were synthesized using the alkoxide–hydroxide route. Formation of BT nanopowders commenced in the specimen synthesized at 60 °C and their amount increased with increasing temperature. However, a TiO_2 second phase was always developed for the specimens synthesized at temperatures above 100 °C. Although the formation of the TiO_2 second phase can be avoided by adding water, it is difficult to control the shape and size of the BT nanopowders formed with water addition. Therefore, in order to synthesize homogeneous, highly tetragonal BT nanopowders without any TiO_2 second phase,

a two-step process was used. The cubic-structure BT nanopowders formed at 100 °C were subsequently heated to high temperatures (>200 °C). The BT nanopowders synthesized at 200 °C for 20 h showed a small c/a ratio of approximately 1.000, with a size of 65.4 nm, and the c/a ratio increased with increasing temperature to 1.0062 for the powders synthesized at 260 °C for 20 h. The c/a ratio and size of the BT nanopowders also increased with increasing heating time. In particular, the BT nanopowders synthesized at 260 °C with a Ba/Ti ratio of 2.0 for 60 h showed a small particles size of 94.8 nm with a high c/a ratio of 1.0081. Therefore, a two-step process using the alkoxide–hydroxide route is a very effective method for the synthesis of small, highly tetragonal BT nanopowders.

Acknowledgement

This research was supported by the research program of Korea University.

References

- [1] D. Hennings, M. Klee, R. Waser, *Adv. Mater.* 3 (1991) 334–340.
- [2] J. Nowotny, M. Rekas, *Solid State Ionics* 49 (1991) 135–154.
- [3] M. Mori, T. Kineri, K. Kadono, T. Sakaguchi, M. Miya, H. Wakabayashi, T. Tsuchiya, *J. Am. Ceram. Soc.* 78 (1995) 2391–2394.
- [4] L.E. Cross, *Am. Ceram. Soc. Bull.* 63 (1984) 585–590.
- [5] P.K. Dutta, J.R. Gregg, *Chem. Mater.* 4 (1992) 843–846.
- [6] J.Q. Ecker, C.C. Hung-Houston, B.I. Gersten, M.M. Lencka, R. Riman, *J. Am. Ceram. Soc.* 79 (1996) 2929–2939.
- [7] A. Testino, M.T. Buscaglia, V. Biscaglia, M. Viviani, C. Bottino, P. Nanni, *Chem. Mater.* 16 (2004) 1536–1543.
- [8] D.F.K. Hennings, C. Metzmacher, B.S. Schreinmacher, *J. Am. Ceram. Soc.* 84 (2001) 179–182.
- [9] S.S. Flaschen, *J. Am. Chem. Soc.* 77 (1955) 6194.
- [10] K. Kiss, J. Meander, M.S. Vukasovich, R.J. Lockhart, *J. Am. Ceram. Soc.* 49 (1996) 291–294.
- [11] J. Qi, L. Li, Y. Wang, Z. Gui, *J. Cryst. Growth* 260 (2004) 551–556.
- [12] N.V. Golubko, M.I. Yanovskaya, L.A. Golubko, E.P. Kovsman, M.B. Listoshina, B.A. Rotenberg, *J. Sol–Gel Sci. Technol.* 20 (2001) 135–143.
- [13] H. Kamiya, K. Gomi, Y. Iida, K. Tanaka, T. Yoshiyasu, T. Kakiuchi, *J. Am. Ceram. Soc.* 86 (2003) 2011–2018.
- [14] S. Yoon, S. Paik, M.G. Kim, N. Shin, *J. Am. Ceram. Soc.* 89 (2006) 1816–1821.
- [15] S. Yoon, S. Paik, M.G. Kim, N. Shin, I. Kim, *J. Am. Ceram. Soc.* 90 (2007) 311–314.
- [16] M.M. Lencka, R.E. Riman, *Chem. Mater.* 5 (1993) 61–70.